Cognitive Neurodynamics (2022) 16:135–147
https://doi.org/10.1007/s11571-021-09710-0

RESEARCH ARTICLE

A new biological central pattern generator model and its relationship with the motor units

Qiang Lu[1] · Xiaoyan Wang[1] · Juan Tian[1]

Received: 1 February 2021 / Revised: 27 June 2021 / Accepted: 31 July 2021 / Published online: 9 August 2021

Abstract

The central pattern generator (CPG) is a key neural-circuit component of the locomotion control system. Recently, numerous molecular and genetic approaches have been proposed for investigating the CPG mechanisms. The rhythm in the CPG locomotor circuits comes from the activity in the ipsilateral excitatory neurons whose output is controlled by interneuron inhibitory connections. Conventional models for simulating the CPG mechanism are complex Hodgkin-Huxley-type models. Inspired by biological investigations and the continuous-time Matsuoka model, we propose new integral-order and fractional-order CPG models, which consider time delays and synaptic interfaces. The phase diagrams exhibit limit cycles and periodic solutions, in agreement with the CPG biological characteristics. As well, the fractional-order model shows state transitions with order variations. In addition, we investigate the relationship between the CPG and the motor units through the construction of integral-order and fractional-order coupling models. Simulations of these coupling models show that the states generated by the three motor units are in accordance with the experimentally-obtained states in previous studies. The proposed models reveal that the CPG can regulate limb locomotion patterns through connection weights and synaptic interfaces. Moreover, in comparison to the integral-order models, the fractional-order ones appear to be more effective, and hence more suitable for describing the dynamics of the CPG biological system.

Keywords Central Pattern Generator · Motor units · Fractional calculus · Synaptic interface

Introduction

The central pattern generator (CPG) is a neural circuit in the brainstem and spinal cord, which constitute the caudal part of the central nervous system in vertebrates. This circuit can generate appropriate muscle activation sequences and control motion in vertebrates, especially mammals (Yang et al. 2017; Bannatyne et al. 2020; Damm et al. 2020). Although the anatomical CPG structure remains largely unclear, many CPG models have been established and applied in robotics for locomotion control(Lu 2015, 2019; McCrea and Rybak 2008; Nassour et al. 2014; Rybak et al. 2006). Two of the most common CPG models are the half-center model (Lu 2015, 2019) and the multi-layered multi-pattern model (McCrea and Rybak 2008; Nassour et al. 2014; Rybak et al. 2006). The half-center model consists of an oscillator with two identical, spontaneously firing neurons. The two neurons are coupled together such that the output of each neuron suppresses the activity of the other. This reciprocal inhibition mechanism is combined with neuron adaptation or fatigue to produce stable oscillations (Lu 2015, 2019). Due to the direct excitatory connections between the rhythm-generating interneurons and the motoneurons, the single-level CPG models couldn't explain the robust locomotion patterns in animals (McCrea and Rybak 2008; Lafreniere-Roula M, McCrea DA 2005). Their investigations showed that the CPG can maintain the locomotor cycle period when motoneurone activity is silent. Such maintenance is incompatible with the single-level half-center CPG structure. Indeed, more sophisticated CPG models were required to manage the adaptation to environmental changes. Therefore, multi-layered CPG models with rhythm-generation and pattern-formation circuits have been proposed

✉ Qiang Lu
luqiang271016@163.com

[1] College of Medical Information Engineering, Shandong First Medical University & Shandong Academy of Medical Sciences, Taian 271000, China

(McCrea and Rybak 2008; Nassour et al. 2014; Rybak et al. 2006). Rybak et al. (2006) proposed two-level CPG organization which can explain the resetting and non-resetting types of deletions observed in fictive locomotion. Nassour et al. (2014) proposed a multi-layered CPG model which can produce various walking patterns and be applied in adaptive robot locomotion. Recently, numerous molecular and genetic approaches have been proposed for investigating the neural circuit organization. Results of these investigations have shown that the basic neural activity patterns for locomotion control in mammals are generated by neural circuits within the spinal cord. These circuits define all aspects of the locomotion activity, including rhythm generation, intralimb flexor–extensor alternation, and left–right limb coordination (Kiehn 2016; Bikoff 2019; Deska-Gauthier and Zhang 2019). These investigations have also shown that the rhythm in a locomotor circuit is generated from neural activity in the ipsilateral excitatory neurons. In fact, both the V1 and V2b interneurons form inhibitory synaptic interfaces with the ipsilateral interneurons, resulting in coordinated flexor–extensor alternations during locomotion. The V1 neurons derived from progenitor cells which express the transcription factor engrailed homeobox 1 (Moran-Rivard et al. 2001) and the V2b neurons that are derived from progenitor cells which express the transcription factor GATA binding protein 2 (Zhou et al. 2000). Based on biological studies of the action mechanisms in the spinal cord, Rybak et al. (2006) have constructed computational models for spinal neuronal circuits. The models described interactions of populations of the Hodgkin-Huxley-type neurons. While these models can explain experimental biological observations, they suffer from structural complexity and low applicability. Compared with the Rybak model, the Matsuoka model (Lu 2015, 2019) is a simple computationally-efficient CPG model but it does not correspond well with biological observations. Motivated by the Rybak and Matsuoka models, we build in this paper a reduced-complexity CPG model that agrees well with biological observations.

In biological locomotion control systems, each motor unit (Bisetto et al. 2019) is an independent functional unit that includes axons, motor neurons (shortened usually to motoneurons), and muscle fibers. Upon activation, the motor unit sends many electrical impulses to the muscle fibers. Also, neurons interact with each other through synaptic connections. By delivering a latent action to presynaptic cells, neurotransmitters will be set out to the postsynaptic cells to activate the receptors on the cell membranes. Nevertheless, although the mammalian locomotion networks have been widely studied, understanding the coupling association in these networks is still an open problem (Kiehn 2016; Roberts et al. 2012). In addition, the relationship between the CPG and the motor cortex has been explored in earlier studies based on the integral-order models (Lu et al. 2015; Lu and Tian 2014) and the fractional-order ones (Lu 2020). The previous investigations showed that there exists parameters space which can make the synchronization of the motor cortex optimum when the CPG is added into the motor cortex. However, the relationship between the CPG and the musculoskeletal system has been rarely explored. According to biological investigations, the CPG controls the basic patterns and rhythms of motoneuron activation during locomotion (Zhong et al. 2018). As well, the CPG has been shown to be tunable by motor neurons and that these motoneurons provide feedback to the CPG (Lawton et al. 2017; Falgairolle et al. 2017). More research on the relationship and association between the CPG and the motor units is warranted to help us understand the underlying interaction mechanisms.

Meanwhile, fractional calculus models of neural systems have emerged, with extended notions of differentiability, non-locality, and memory effects via time derivatives and fractional-order spaces (Teka et al. 2017). Based on these fractional calculus tools, a complex system can be modeled using multiple space and time scales without subdivision into many smaller subsystems (Lin et al. 2018). Fractional calculus has already been applied in different areas, especially neural system modeling (Qiao et al. 2020; Chen et al. 2020; Yan et al. 2017). Qiao et al. (2020) investigated finite-time synchronization of fractional-order gene regulatory networks with time delay. Chen et al. (2020) proposed fractional-order discrete Hopfield neural networks, and studied the dynamic behavior and applications of these networks. Neural networks can account for the features of fractional-order systems and complex neuronal dynamics (Qiao et al. 2020; Chen et al. 2020; Yan et al. 2017). According to the biological investigations, the core part of the CPG and motor units are neurons (Moran-Rivard et al. 2001; Bisetto et al. 2019). And the researchers (Lundstrom et al. 2008) found the neuron has the multiple time scale adaptation which is compatible with the fractional calculus. As microscopic neural networks, the CPG and motor units should possess the characteristics of fractional-order systems. Hence, we investigate in this work fractional-order CPG models, motor units, and their coupling models.

The rest of this paper is arranged as follows. In Sect. Proposed model for the CPG and motor units, the integral-order and fractional-order CPG models, motor units with time delay, and synaptic interfaces are studied. Section Models of coupling between the CPG and motor units shows the integral-order and fractional-order coupling models with computer simulations. In Sect. Conclusions, conclusions are drawn and future research directions are highlighted.

Proposed model for the CPG and motor units

Biological CPG model

According to experimental biological observations, a CPG contains rhythm generators with flexor and extensor centers that inhibit each other via inhibitory interneuron populations (Kiehn 2016; Bikoff 2019; Deska-Gauthier and Zhang 2019; Shevtsova et al. 2015). A mathematical CPG model is typically constructed as a continuous-time continuous-variable model (Matsuoka 2011). Based on the above description, we establish a new simplified CPG model as shown in Fig. 1.

In Fig. 1, the filled black circles indicate inhibitory actions while the unfilled circles represent excitatory actions. The node variables $x_i(i = 1, 2, 3, 4)$ represent membrane potentials. The parameters T_r and e denote the time constant and tonic input, respectively. w represents the strength among the neurons.

Hence, the simplified CPG model can be described by

$$\begin{cases} T_r \dot{x}_1 = x_1 - wx_4 + e \\ T_r \dot{x}_2 = x_2 - wx_3 + e \\ T_r \dot{x}_3 = -x_3 + wx_1 \\ T_r \dot{x}_4 = -x_4 + wx_2 \end{cases} \tag{1}$$

The values of T_r for all neurons are identical. The tonic inputs e for x_1 and x_2 are the same. The values of w in Eq. 1 are identical and positive. The output of the CPG model is x_1. The model parameters are set as $T_r = 1$, $e = 0$, and $w = 2.5$. The initial values of the membrane potentials are set as $[0.1 \quad 0.1 \quad 0.1 \quad 0.1]$. The output and phase diagram of this CPG model are shown in Fig. 2.

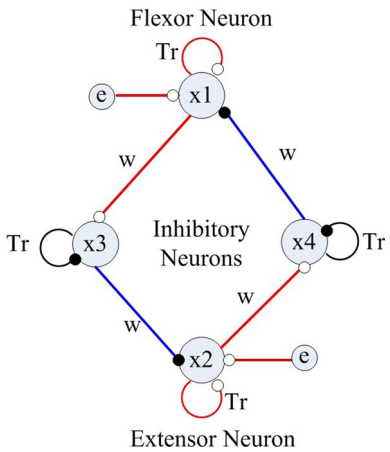

Fig. 1 The simplified CPG model

In Fig. 2(b), the phase plane shows a limit cycle which is a typical CPG pattern. Thus, the simplified CPG model is in accordance with the CPG biological structure and work mechanism. Moreover, time delays play an important role in neural networks (He et al. 2020). In the following, the above mentioned CPG model is augmented with a time delay component.

The impulse-response function $h_d(t)$ of a time delay (Lu 2015) is given by

$$h_d(t) = \begin{cases} Aa_d t e^{-a_d t} (t \geq 0) \\ 0 (t < 0) \end{cases} \tag{2}$$

where A denotes the maximal amplitude of the postsynaptic potentials, and the parameter a_d lumps together the characteristic delays of synaptic transmission. If the input is $m(t)$, then the output is $y(t) = h_d * m(t)$, where the symbol $*$ denotes the convolution operator.

The present model can be described mathematically as a second-order ordinary differential equation

$$\ddot{y}(t) = Aa_d m(t) - 2a_d \dot{y}(t) - a_d^2 y(t) \tag{3}$$

which can also be rewritten as a system of two first-order differential equations,

$$\begin{cases} \dot{y}(t) = z(t) \\ \dot{z}(t) = Aa_d m(t) - 2a_d z(t) - a_d^2 y(t) \end{cases} \tag{4}$$

According to Eq. 1, $x_i(t)(i = 1, ..., 4)$ are replaced by $m_i(t)(i = 3, ..., 6)$, respectively. $y(t)$ and $z(t)$ are replaced by $m_1(t)$ and $m_2(t)$ based on Eq. 4, respectively. Using the CPG output $m_3(t)$ as the input of Eq. 4, the state equations of the new CPG model with time delay are given by

$$\begin{cases} \dot{m}_1 = m_2 \\ \dot{m}_2 = Aa_d m_3 - 2a_d m_2 - a_d^2 m_1 \\ T_r \dot{m}_3 = m_3 - wm_6 + e \\ T_r \dot{m}_4 = m_4 - wm_5 + e \\ T_r \dot{m}_5 = -m_5 + wm_3 \\ T_r \dot{m}_6 = -m_6 + wm_4 \end{cases} \tag{5}$$

Furthermore, neurons interact with each other at synaptic interfaces. The capacity of pre-synaptic cells for sending out neurotransmitters is called the pre-synaptic strength, which is denoted here by s. This strength is modeled by the kinetic equation

$$\dot{s} = \eta(1 - s)s_\infty(x) - \beta s \tag{6}$$

where

$$s_\infty(x) = \frac{1}{1 + e^{-(x-\theta_s)/k_s}} \tag{7}$$

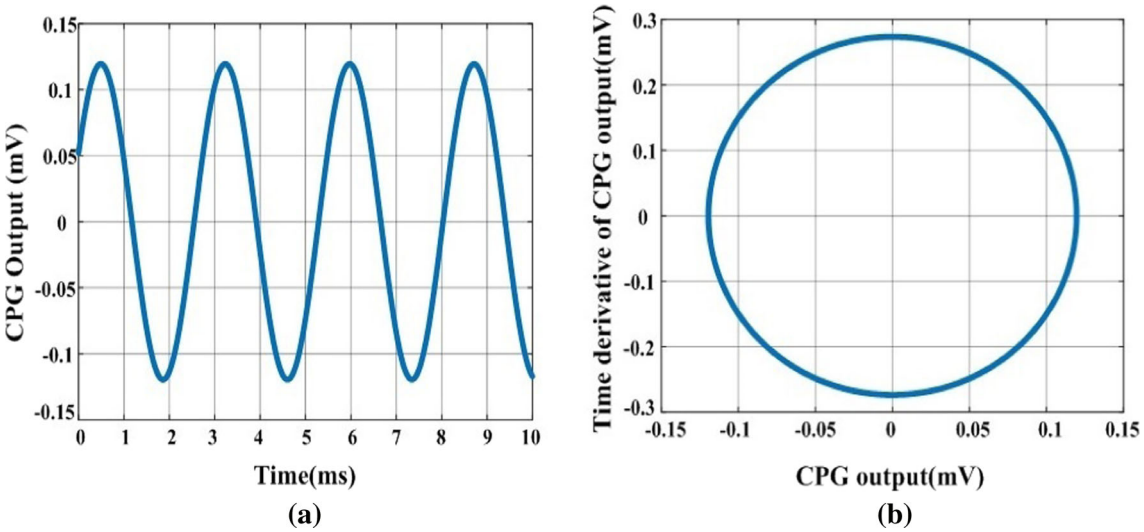

Fig. 2 Simulation outcomes of the simplified CPG model: **a** model output, **b** phase plane

In Eqs. 6 and 7, x denotes the pre-synaptic voltage, k_s represents the steepness, θ_s represents the threshold value at which the function is half-activated, while η and β denote voltage-independent rate constants.

Based on the receptor and neurotransmitter types, transitions in the neuron states can occur. These transitions can be modeled as a synaptic current flowing to the post-synaptic cells (Bisetto et al. 2019):

$$I_{syn} = sg_{syn}(V - V_{syn}) \tag{8}$$

where I_{syn} denotes the net synaptic current and the parameter s denotes the pre-synaptic strength. The parameter g_{syn} represents the post-synaptic conductance, and V_{syn} represents the reversal potential for the synaptic current. Then, a new model of neuron dynamics with synaptic transmission can be established as

$$\begin{cases} \dot{m}_1 = m_2 \\ \dot{m}_2 = Aa_d m_3 - 2a_d m_2 - a_d^2 m_1 \\ T_r \dot{m}_3 = m_3 - wm_6 + e + I_{syn} \\ T_r \dot{m}_4 = m_4 - wm_5 + e + I_{syn} \\ T_r \dot{m}_5 = -m_5 + wm_3 \\ T_r \dot{m}_6 = -m_6 + wm_4 \\ \dot{s} = \eta(1 - s)s_\infty(m_1) - \beta s \end{cases} \tag{9}$$

Next, we introduce a fractional-order neuron model. In this work, we use the Grunwald–Letnikov (G-L) fractional derivative (Lu 2019, 2020), and obtain the following fractional-order CPG model with synaptic transmission,

$$\begin{cases} {}^{GL}D^{\alpha} m_1 = m_2 \\ {}^{GL}D^{\alpha} m_2 = Aa_d m_3 - 2a_d m_2 - a_d^2 m_1 \\ {}^{GL}D^{\alpha} m_3 = (m_3 - wm_6 + e + I_{syn})/T_r \\ {}^{GL}D^{\alpha} m_4 = (m_4 - wm_5 + e + I_{syn})/T_r \\ {}^{GL}D^{\alpha} m_5 = (-m_5 + wm_3)/T_r \\ {}^{GL}D^{\alpha} m_6 = (-m_6 + wm_4)/T_r \\ {}^{GL}D^{\alpha} s = \eta(1 - s)s_\infty(m_1) - \beta s \end{cases} \tag{10}$$

where ${}^{GL}D^{\alpha}$ represents the G-L fractional derivative operator, and α is a non-integer number that represents the fractional order. And the output is m_1.

We performed several simulations of the proposed fractional-order model. In these simulations, the order α is chosen at equally spaced values within the range $[0.7, 0.97]$ with a step of 0.03. The other model parameters are set as: $\theta_s = -37mV$, $I_{syn} = 0\mu A$, $k_s = 2$, $a_d = 4$, $\eta = 2$, and $\beta = 0.03$. Phase diagrams of this fractional-order CPG model are shown in Fig. 3 for different values of α.

In Fig. 3, the main figure shows the phase diagram of the fractional-order CPG model when the order α is in the range $[0.7, 0.97]$. The three small figures show the phase diagrams for fractional orders of 0.7, 0.82 and 0.97, respectively. Figure 3 shows memory and hereditary characteristics of fractional-order systems. The researches (Lundstrom et al. 2008) showed that the neuron has the multiple time scale adaptation which can be described by the fractional calculus. The parameter α represents the time scale. With the change of the variable α, the phase diagram shows the evolution of the CPG pattern with different time scales. Obviously, when the new CPG model with synaptic transmission is extended to the fractional-order domain, the

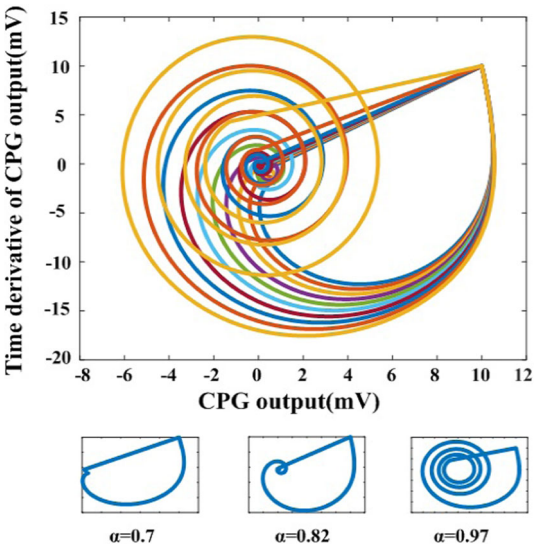

Fig. 3 Phase planes for a fractional-order CPG model at different fractional orders

extended model shows clear variations with the fractional order.

The FitzHugh-Nagumo motor unit model with time delay and synaptic transmission

Motor units have been conventionally modeled by the Hodgkin-Huxley model which can be formulated as a large system of differential equations (Bisetto et al. 2019). In order to obtain a motor unit model with reduced structural complexity, the FitzHugh-Nagumo (FN) model (Kumar et al. 2018; Ge et al. 2020) has been adopted. This is a simplified variant of the Hodgkin-Huxley model for describing the transmission of nerve impulses. The FN model is described as

$$\begin{cases} V^{\bullet} = c(V - \dfrac{V^3}{3} + \lambda + I_c) \\ \dot{\lambda} = -\dfrac{1}{c}(V - a + b\lambda) \end{cases} \tag{11}$$

where V and λ are the voltage variable and recovery variable, respectively. I_c is the external stimulus. a, b and c are constants.

When time delays are considered, $y(t)$ and $z(t)$ are replaced by V_1 and V_2 based on Eq. 4, respectively. We obtain the state equations

$$\begin{cases} \dot{V}_1 = V_2 \\ \dot{V}_2 = Aa_dV - 2a_dV_2 - a_d^2V_1 \\ \dot{V} = c(V - \dfrac{V^3}{3} + \lambda + I_c) \\ \dot{\lambda} = -\dfrac{1}{c}(V - a + b\lambda) \end{cases} \tag{12}$$

In addition, if synaptic interfaces and transmission are accounted for, we obtain the integral-order model

$$\begin{cases} \dot{V}_1 = V_2 \\ \dot{V}_2 = Aa_dV - 2a_dV_2 - a_d^2V_1 \\ \dot{V} = c(V - \dfrac{V^3}{3} + \lambda + I_c) \\ \dot{\lambda} = -\dfrac{1}{c}(V - a + b\lambda) \\ \dot{s} = \eta(1 - s)s_\infty(V_1) - \beta s \end{cases} \tag{13}$$

Moreover, the corresponding fractional-order model can be obtained as

$$\begin{cases} {}^{GL}D^{\alpha}V_1 = V_2 \\ {}^{GL}D^{\alpha}V_2 = Aa_dV - 2a_dV_2 - a_d^2V_1 \\ {}^{GL}D^{\alpha}V = c(V - \dfrac{V^3}{3} + \lambda + I_c) \\ {}^{GL}D^{\alpha}\lambda = -\dfrac{1}{c}(V - a + b\lambda) \\ {}^{GL}D^{\alpha}s = \eta(1 - s)s_\infty(V_1) - \beta s \end{cases} \tag{14}$$

And the output is V_1. In the following simulations, the fractional order α is chosen at equally-spaced points within the range $[0.7, 0.97]$ with a step of 0.03. The other model parameters are set as $\theta_s = -37mV$, $k_s = 2$, $a_d = 4$, $a = 0.7$, $b = 0.8$, $c = 3$, $I_c = -1$, $\eta = 2$ and $\beta = 0.03$. Phase diagrams of the integral-order and fractional-order FN models are shown in Fig. 4.

Figure 4(a) shows the phase-plane diagram of the integral-order FN model, while Fig. 4(b) shows phase-plane diagrams of the fractional-order FN model for different fractional-order values α in the range $[0.7, 0.97]$. The three small phase diagrams in Fig. 4(b) correspond to fractional orders of 0.7, 0.82, and 0.97, respectively. Also, the phase diagrams of Fig. 4 are of the limit-cycle type. This remark verifies the concordance between the new FN models and biological neuron behavior. In comparison to the integral-order FN model, the fractional-order FN models show richer system dynamics and parameter-dependent state transitions.

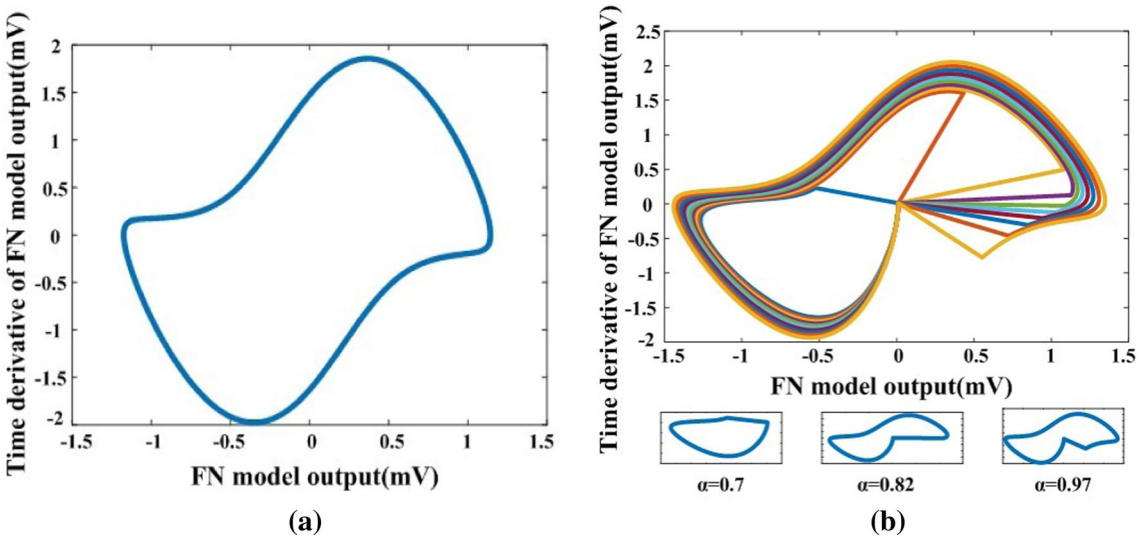

Fig. 4 Phase-plane diagrams of the integral-order and fractional-order FN models of motor units: **a** Integral-order FN model, **b** Fractional-order FN model

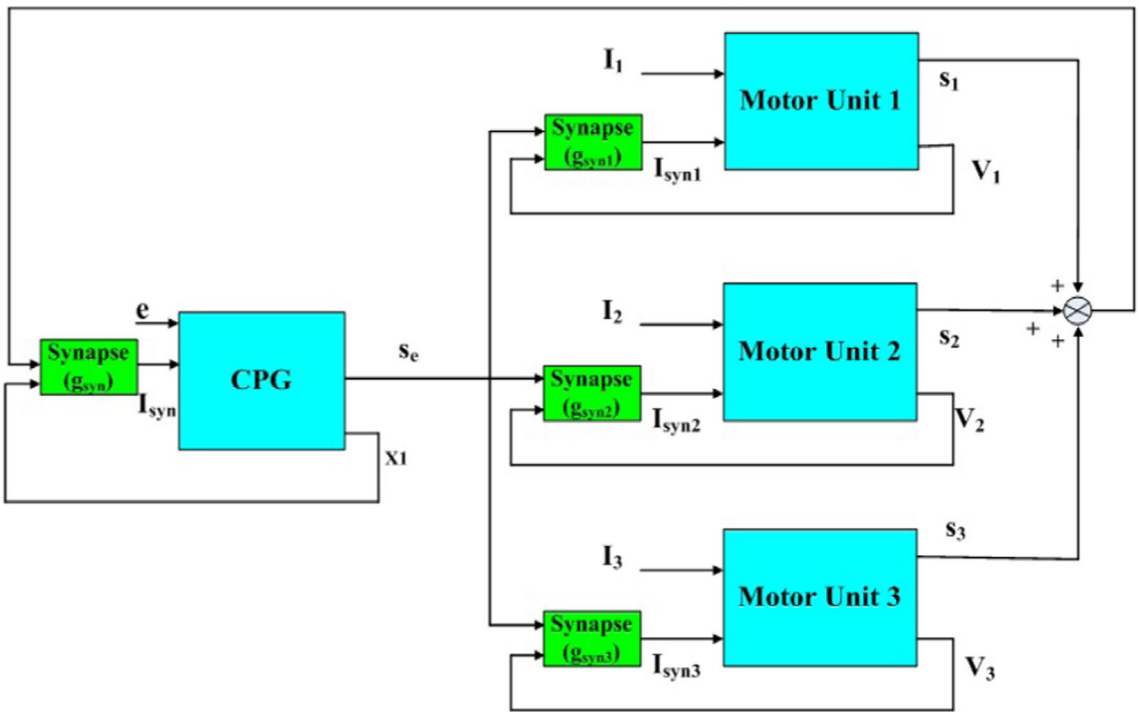

Fig. 5 A block diagram of the proposed model of coupling between the CPG and the motor units

Models of coupling between the CPG and motor units

The CPG can control the states of the motor neurons, while these neurons can provide feedback and tune the CPG output (Zhong et al. 2018; Lawton et al. 2017; Falgairolle et al. 2017). Based on these biological observations, we build a model for the coupling between the CPG and the motor units as shown in Fig. 5.

In Fig. 5, an integral-order (or a fractional-order) CPG model with synapses is shown on the left. On the right, blocks are shown for three motor units. Each motor unit has one motor neuron, which is represented by an integral-order (or a fractional-order) FN model. The CPG model output s_e is sent to the three motor units, while the summation of the outputs of these three units is fed back to the CPG model. The synaptic conductance parameters of the

CPG and the three units are denoted by g_{syn}, g_{syn1}, g_{syn2} and g_{syn3}, respectively.

Here, the dynamic relation between the motor units and the CPG is investigated under two CPG models, namely the integral-order and the fractional-order CPG models. Conclusions are drawn based on simulations of the two models.

Coupling relationship between the integral-order CPG model and the motor units

The CPG has shown the capability to generate motor rhythm signals and distribute them to different motor units through flexible weights (Lacquaniti et al. 2012; Dominici et al. 2011; Ivanenko et al. 2005). In the following simulations, the CPG synaptic conductance g_{syn} is set to 0.01, while that of one motor unit g_{syn1} is chosen uniformly within the range of $[0.01, 0.1]$ with a step of 0.01. For the two other units, the synaptic conductance values of g_{syn2} and g_{syn3} are set to 0.02 and 0.05, respectively. The motor unit patterns generated based on the integral-order CPG model are shown in Fig. 6.

In Fig. 6, the synaptic conductance values, g_{syn}, g_{syn2} and g_{syn3}, are fixed. As g_{syn1} is varied, different patterns are generated by the three motor units. The simulation results verify the CPG ability to regulate the motor unit states. This result is in accordance with earlier investigations (Lacquaniti et al. 2012; Dominici et al. 2011; Ivanenko et al. 2005). These earlier investigations showed that the CPG control the basic rhythms and patterns of motoneuron activation during locomotion. In these investigations, the researchers used three body parts to establish different patterns. In Fig. 6, the patterns are generated by the three motor units. If the motor units are located in different body parts, the coupling model can be used to expound the biological phenomena.

Next, we assess the effects of different feedback weights on the CPG output through varying the value of the CPG synaptic conductance g_{syn}. In the following simulations,

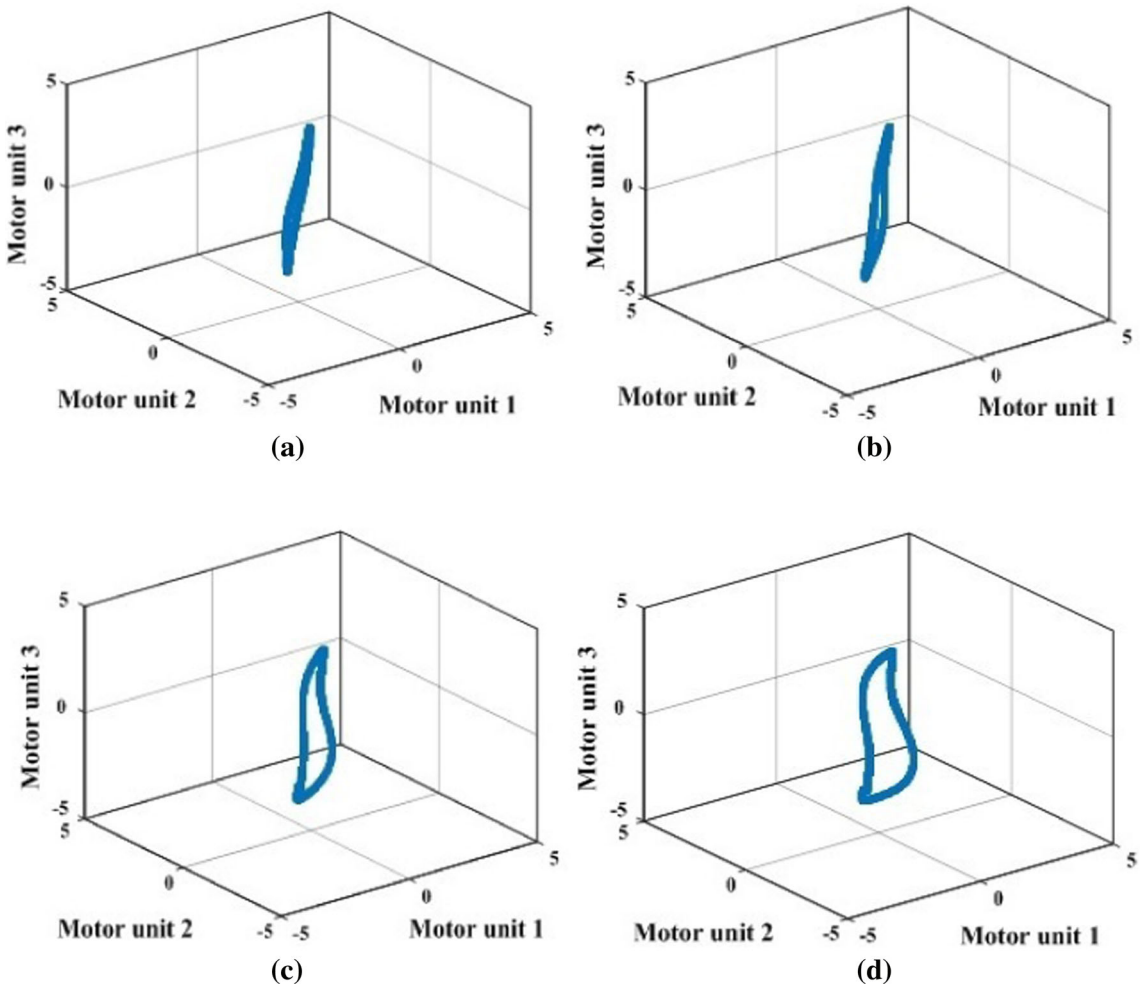

Fig. 6 Motor unit patterns generated based on the integral-order CPG model with different values of g_{syn1} while the other synaptic conductance parameters are fixed: **a** $g_{syn1} = 0.01$, **b** $g_{syn1} = 0.04$, **c** $g_{syn1} = 0.07$, **d** $g_{syn1} = 0.1$

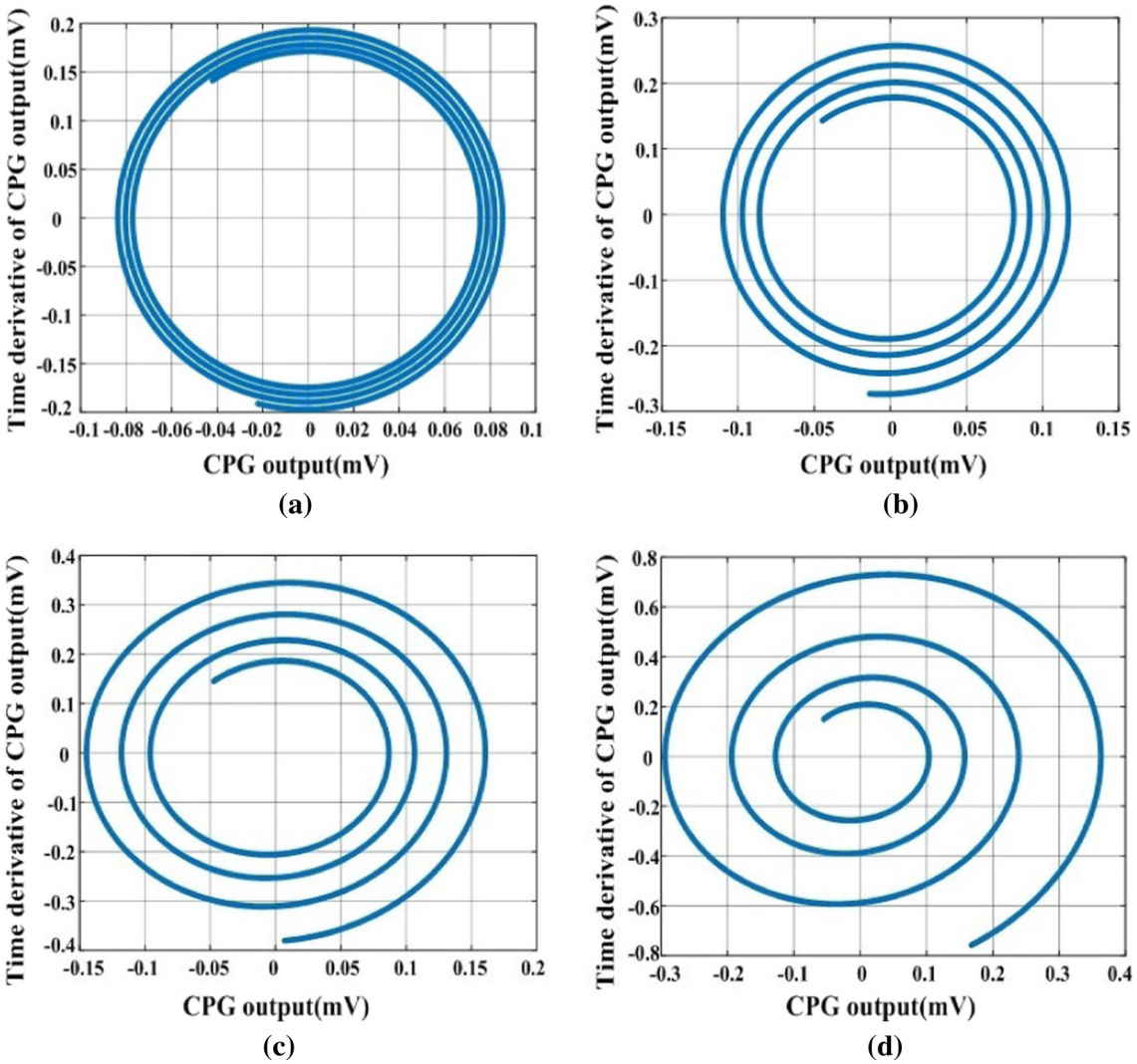

Fig. 7 Phase diagrams of the integral-order coupling model with different values of g_{syn} while other conductance parameters are fixed: **a** $g_{syn} = 0.01$, **b** $g_{syn} = 0.03$, **c** $g_{syn} = 0.05$, **d** $g_{syn} = 0.1$

this conductance is chosen uniformly within the range of $[0.01, 0.1]$ with a step of 0.01. The values of the other conductance parameters, g_{syn1}, g_{syn2} and g_{syn3}, are set to 0.01, 0.02, and 0.05, respectively. The phase-plane diagrams for the integral-order coupling model and different values of g_{syn} are shown in Fig. 7.

In Fig. 7, the phase diagram of the integral-order coupling model varies with different values of g_{syn}. Although the results demonstrate that the CPG output can be affected by motor neurons, the phase diagram is not of the limit-cycle type. Therefore, the integral-order coupling model can't adequately explain the CPG dynamics.

Coupling relationship between the fractional-order CPG model and the motor units

Now, we evaluate the effectiveness of the fractional-order models in capturing the coupling between the CPG and motor units. In the following simulations, g_{syn1} is chosen uniformly within the range $[0.01, 0.1]$ with a step of 0.01. The values of the other conductance parameters, g_{syn}, g_{syn2} and g_{syn3}, are set to 0.01, 0.02, and 0.05, respectively. The fractional order α is chosen uniformly within the range $[0.7, 0.97]$ with a step of 0.03. Figure 8 shows the motor neuron patterns generated by the different fractional-order coupling models.

In Fig. 8, the patterns generated by the three fractional-order motor units are plotted with different α and g_{syn1} values. The three small diagrams in each subfigure are the phase diagrams for fractional orders of 0.7, 0.82, and 0.97,

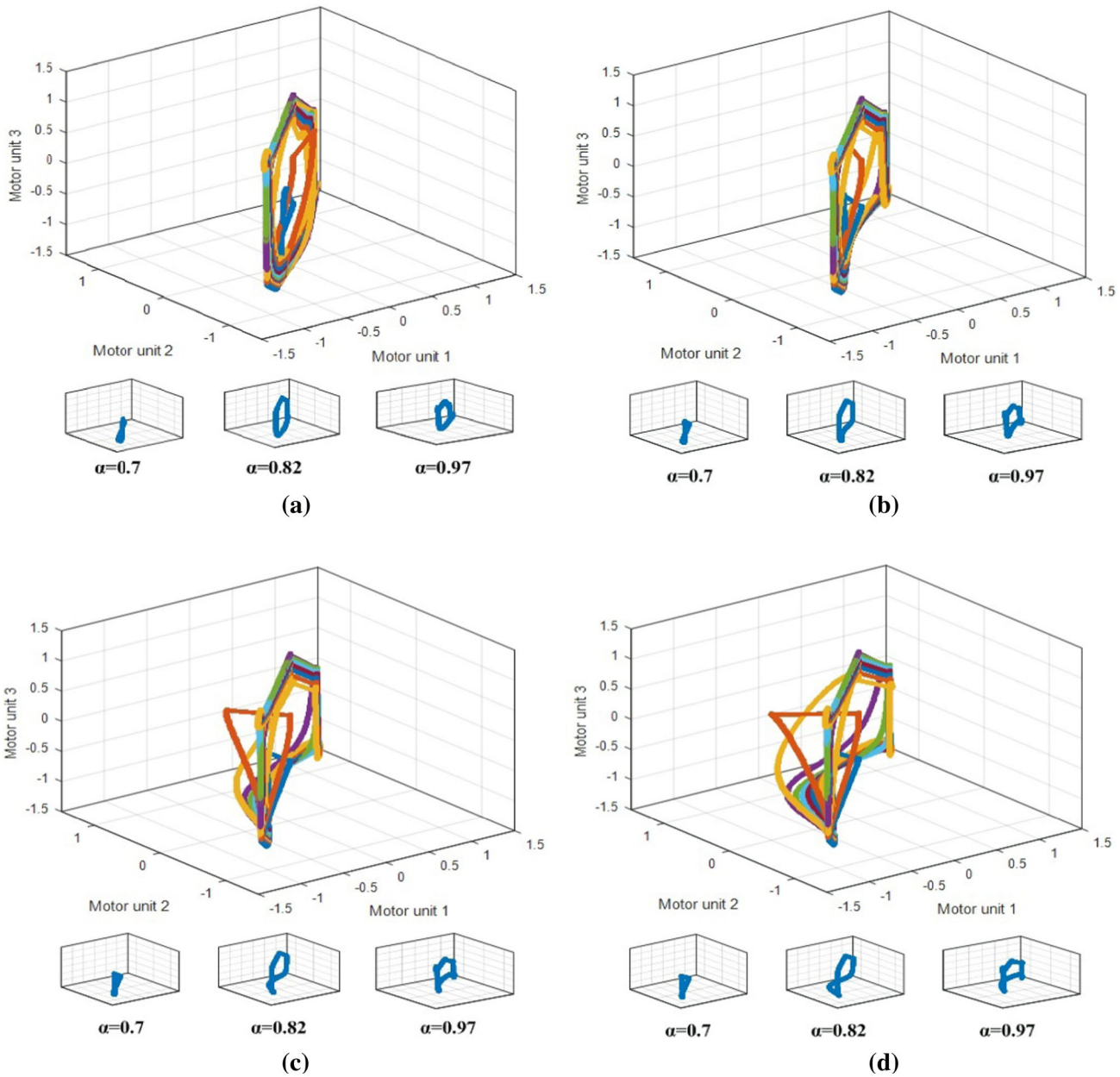

Fig. 8 Motor neuron patterns generated by fractional-order coupling models with different values of g_{syn1} while other conductance parameters are fixed: **a** $g_{syn1} = 0.01$, **b** $g_{syn1} = 0.04$, **c** $g_{syn1} = 0.07$, **d** $g_{syn1} = 0.1$

respectively. The results confirm that locomotion patterns can be tuned by the CPG through different weights. The phase diagrams also show state transitions with fractional-order variations. The fractional-order coupling models are clearly more effective than the integral-order one.

In addition, we investigate the effects of varying the feedback weights on the fractional-order CPG model output. In particular, we vary the value of g_{syn} uniformly within the range $[0.01, 0.1]$ with a step of 0.01. The values of the other conductance parameters, g_{syn1},g_{syn2} and g_{syn3}, are chosen as 0.01, 0.02, and 0.05, respectively. The fractional order α is selected uniformly from the range $[0.7, 0.97]$ with a step of 0.03. The CPG patterns generated based on the motor unit feedback are shown in Fig. 9.

In Fig. 9, the states vary with the change in the g_{syn} values based on the fractional-order coupling model. This is especially evident for the fractional order of 0.97. The simulations demonstrate that the CPG state can be affected by firings from the fractional-order motor neurons. This remark is in agreement with biological observations (Lawton et al. 2017; Falgairolle et al. 2017; Teka et al. 2017). The fractional-order coupling models exhibit phase diagrams of the limit-cycle type, while an integral-order

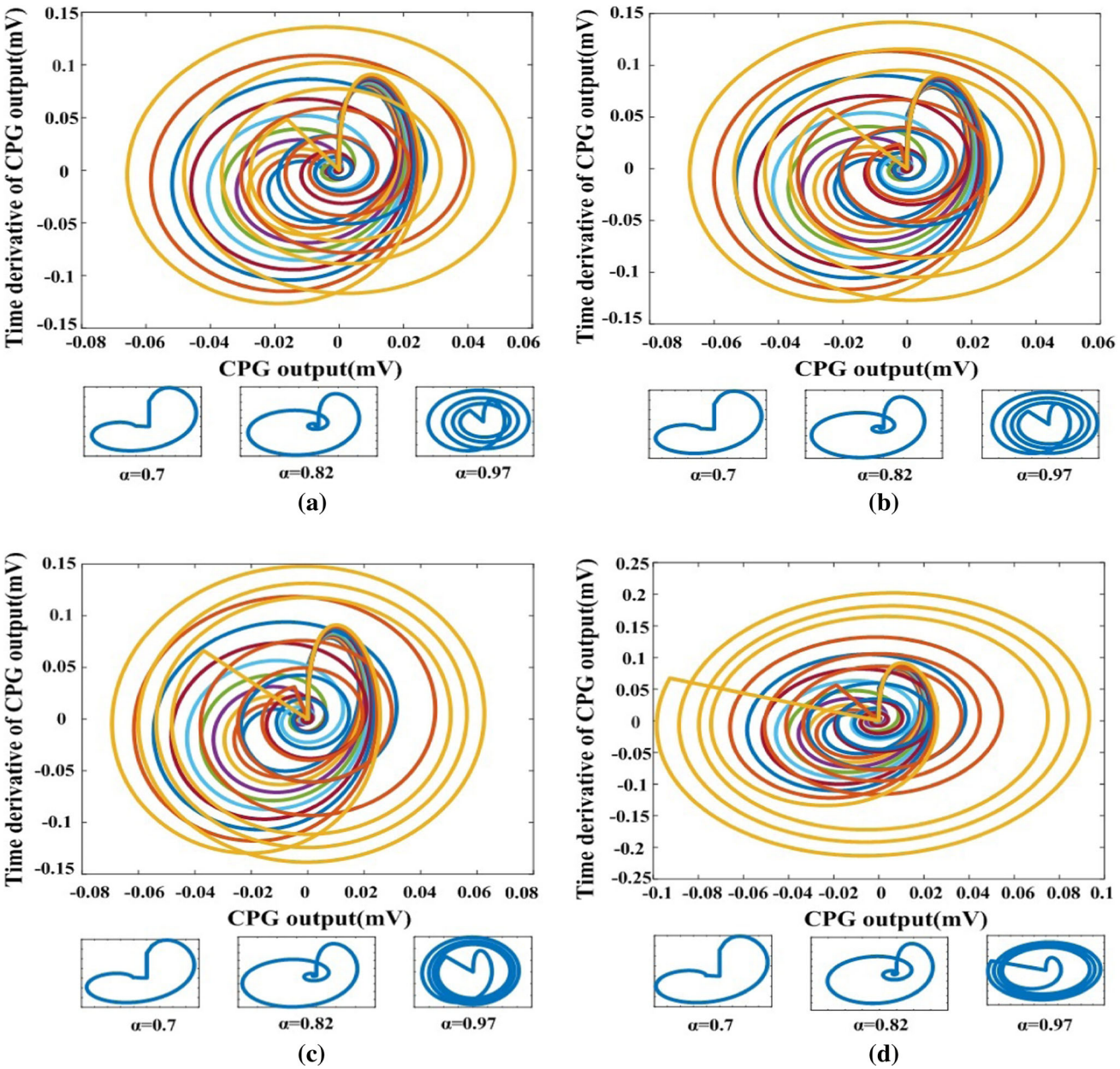

Fig. 9 Phase diagrams of the fractional-order coupling model with different values of g_{syn} while other conductance parameters are fixed: **a** $g_{syn} = 0.01$, **b** $g_{syn} = 0.03$, **c** $g_{syn} = 0.05$, **d** $g_{syn} = 0.1$

model doesn't. Therefore, fractional-order coupling models can describe neural coupling relationships more faithfully.

Finally, we analyze the effect of varying the time-delay parameter a_d on the CPG output with fractional-order coupling models. The values of the conductance parameters g_{syn},g_{syn1},g_{syn2} and g_{syn3} are selected as 0.05, 0.01, 0.02, and 0.05 respectively. The order α is again selected uniformly in the range $[0.7, 0.97]$ with a step of 0.03. The time-delay parameter a_d is chosen uniformly within the range $[1, 10]$ with a step of 1. The simulation results are shown in Fig. 10.

In Fig. 10, the CPG states of the fractional-order coupling model clearly vary with the change in the values of the time-delay parameter a_d(Lu 2015). Similar simulations with the integral-order coupling model show no significant effects on the CPG states. Therefore, fractional-order models are more suitable than the integral-order one for describing the coupling relations in neural systems.

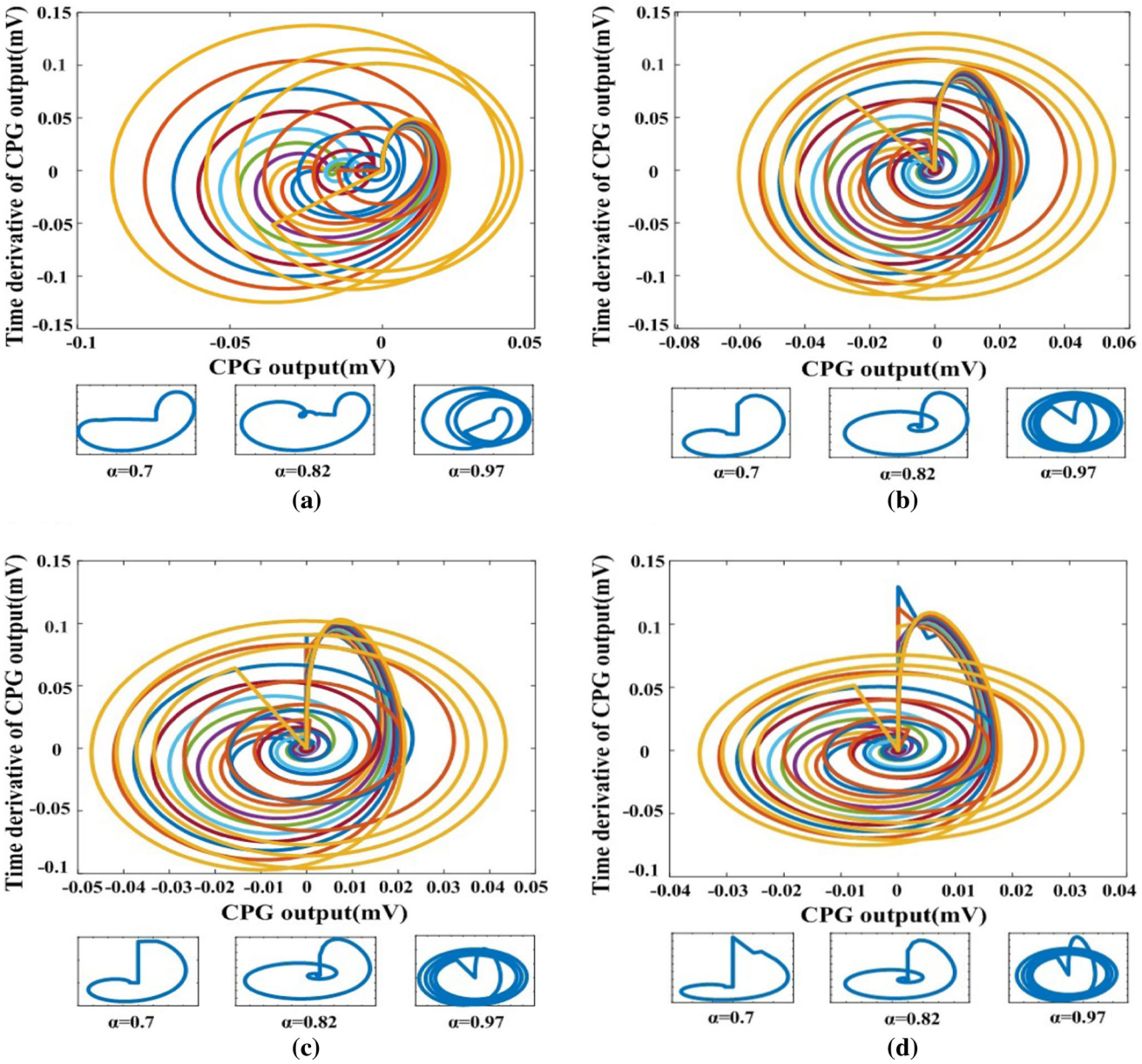

Fig. 10 Phase diagrams of the fractional-order coupling model with different values of the time-delay parameter a_d and the fractional order α: **a** $a_d = 1$, **b** $a_d = 5$, **c** $a_d = 7$, **d** $a_d = 10$

Conclusions

In this paper, a new simplified CPG model that agrees with known biological mechanisms has been proposed. The model has also been augmented by time-delay and fractional-calculus components to reflect the rich dynamic characteristics of neural systems. The proposed model does not only possess the biological structure of neural oscillators, but it also involves just a few state equations. As well, our model combines the features of the Rybak and Matsuoka models (Lu 2019, 2015; Shevtsova et al. 2015). Moreover, a FN model of motor units has been established where synaptic transmission and time delays have been accounted for. Consequently, new integral-order and fractional-order models have been built to capture the coupling between the motor units and the CPG. Through simulations, the proposed models exhibited rich dynamic characteristics that could help in capturing the relation between the CPG and the motor units. Because a motor unit is the functional unit that directly connects with muscle fibers, the simulations indicate that the locomotion patterns could be controlled through the CPG by proper connection weights. Meanwhile, the results also demonstrate that the feedback from the motor units can influence the CPG

output via synaptic connections. We demonstrate that the proposed models are effective and can be used to explain relevant biological phenomena. Nevertheless, the fractional-order coupling models show better and more truthful performance compared to the integral-order one.

In conclusion, some key remarks on the afore-mentioned models are as follows. First, the new CPG model is established according to biological observations (Kiehn 2016; Bikoff 2019; Deska-Gauthier and Zhang 2019; Shevtsova et al. 2015). And the model generates the typical feature of the limit cycle. The simulations are in agreement with biological observations (Lawton et al. 2017; Falgairolle et al. 2017; Teka et al. 2017). The build process of CPG model is consistent with the process of other CPG models (Matsuoka 2011; Nassour et al. 2014). Compare with the classical Hodgkin-Huxley-type models for simulating the CPG mechanism, the new integral-order and fractional-order CPG models are simple and effective. Second, although only three motor neurons have been used in the simulations, the results show that the patterns generated by these neurons are similar to those obtained by earlier models (Lacquaniti et al. 2012; Dominici et al. 2011; Ivanenko et al. 2005). In these investigations, the researchers used the thigh angle versus shank and foot angles to show different patterns which are the intersegmental coordination of motor units. In Figs. 6 and 8, the patterns are generated by the three motor units and are in accordance with previous investigations. If the motor units are located in the thigh, shank and foot, the coupling model can be used to explain the underlying biological phenomena. Hence, the proposed models are effective. When the CPG connects with the motor units through synapses, the CPG can tune the locomotion patterns generated by the motor units. Third, the researchers (Lundstrom et al. 2008) found the neuron has the multiple time scale adaptation which is compatible with the fractional calculus. Therefore, the fractional-order models are more suitable than the integral-order one for describing the coupling relations in neural systems. The CPG, motor units, and their coupling model can be better investigated through fractional-calculus tools. Hence, our work not only verifies the relation between the CPG and the motor units in neural systems, but also provides novel approaches for locomotion control.

In neural systems, oscillations (or rhythms) are observed across various temporal and spatial scales. Such oscillations play important roles in neural communication and computation (Fiebelkorn and Kastner 2019; Fries 2015). One prominent theory is that oscillations accomplish such functions using cross-frequency coupling (Cole and Voytek 2017). The CPG is a rhythm oscillator which can modulate the locomotion patterns and exhibit different frequencies. Therefore, biological connections and cross-frequency coupling between the motor cortex, the CPG, and the motor units are deserved to be explored and investigated further.

Acknowledgements This work was supported by the Key Research and Development Project of Shandong Province in China under Grant 2019GGX101062, and Shandong Provincial Natural Science Foundation, China under Grant ZR2020MF156.

References

Bannatyne BA, Hao ZZ, Dyer GMC et al (2020) Neurotransmitters and motoneuron contacts of multifunctional and behaviorally specialized turtle spinal cord interneurons. J Neurosci 40(3):2680–2694

Bikoff JB (2019) Interneuron diversity and function in the spinal motor system. Curr Opin Physio 8:36–43

Bisetto S, Wright MC, Nowak RA, et al. (2019) New insights into the lactate shuttle: role of MCT4 in the modulation of the exercise capacity. iScience 22: 507.

Chen L, Hao Y, Huang T et al (2020) Chaos in fractional-order discrete neural networks with application to image encryption. Neural Netw 125:174–184

Cole SR, Voytek B (2017) Brain oscillations and the importance of waveform shape. Trends Cogn Sci 21(2):137–149

Damm L, Varoqui D, De Cock VC et al (2020) Why do we move to the beat? a multi-scale approach, from physical principles to brain dynamics. Neurosci Biobehav Rev 112:553–584

Deska-Gauthier D, Zhang Y (2019) The functional diversity of spinal interneurons and locomotor control. Curr Opin Physio 8:99–108

Dominici N, Ivanenko YP, Cappellini G et al (2011) Locomotor primitives in newborn babies and their development. Science 334(6058):997–999

Falgairolle M, Puhl JG, Pujala A, et al. (2017). Motoneurons regulate the central pattern generator during drug-induced locomotor-like activity in the neonatal mouse. eLife 6: e26622.

Fiebelkorn IC, Kastner S (2019) A rhythmic theory of attention. Trends Cogn Sci 23(2):87–101

Fries P (2015) Rhythms for cognition: communication through coherence. Neuron 88:220–234

Ge MY, Lu LL, Xu Y et al (2020) Vibrational mono-bi/-resonance and wave propagation in FitzHugh-Nagumo neural systems under electromagnetic induction. Chaos Solitons Fractals 133:109645

He WM, Ahn CK, Xiang ZR (2020) Global fault-tolerant sampled-data control for large-scale switched time-delay nonlinear systems. IEEE Syst J 14(2):1549–1557

Ivanenko YP, Cappellini G, Dominici N et al (2005) Coordination of locomotion with voluntary movements in humans. J Neurosci 25(31):7238–7253

Kiehn O (2016) Decoding the organization of spinal circuits that control locomotion. Nat Rev Neurosci 17:224–238

Kumar D, Singh J, Baleanu D (2018) A new numerical algorithm for fractional Fitzhugh-Nagumo equation arising in transmission of nerve impulses. Nonlinear Dyn 91(1):307–317

Lacquaniti F, Ivanenko YP, Zago M (2012) Patterned control of human locomotion. J Physiol 590(10):2189–2199

Lafreniere-Roula M, McCrea DA (2005) Deletions of rhythmic motoneuron activity during fictive locomotion and scratch provide clues to the organization of the mammalian central pattern generator. J Neurophysiol 94(2):1120–1132

Lawton KJ, Perry WM, Yamaguchi A et al (2017) Motor neurons tune premotor activity in a vertebrate central pattern generator. J Neurosci 37(12):3264–3275

Lin L, Zheng L, Chen Y et al (2018) Anomalous diffusion in comb model with fractional dual-phase-lag constitutive relation. Comput Math Appl 76(2):245–256

Lu Q (2015) Coupling relationship between the central pattern generator and the cerebral cortex with time delay. Cogn Neurodyn 9:423–436

Lu Q (2019) Relationship between the nonlinear oscillator and the motor cortex. IEEE Access 7:44525–44535

Lu Q (2020) Dynamics and coupling of fractional-order models of the motor cortex and central pattern generators. J Neural Eng 17:036021

Lu Q, Tian J (2014) Synchronization and stochastic resonance of the small-world neural networks based on the CPG. Cogn Neurodyn 8(3):217–226

Lu Q, Li W, Tian J et al (2015) Effects on hypothalamus when CPG is fed back to basal ganglia based on KIV model. Cogn Neurodyn 9(1):85–92

Lundstrom BN, Higgs MH, Spain WJ et al (2008) Fractional differentiation by neocortical pyramidal neurons. Nat Neurosci 11:1335–1342

Matsuoka K (2011) Analysis of a neural oscillator. Biol Cybern 104:297–304

McCrea DA, Rybak IA (2008) Organization of mammalian locomotor rhythm and pattern generation. Brain Res Rev 57(1):134–146

Moran-Rivard L, Kagawa T, Saueressig H et al (2001) Evx1 is a postmitotic determinant of v0 interneuron identity in the spinal cord. Neuron 29(2):385–399

Nassour J, Henaff P, Benouezdou F et al (2014) Multi-layered multi-pattern CPG for adaptive locomotion of humanoid robots. Biol Cybern 108:291–303

Qiao Y, Yan H, Duan L et al (2020) Finite-time synchronization of fractional-order gene regulatory networks with time delay. Neural Netw 126:1–10

Roberts A, Li WC, Soffe SR (2012) A functional scaffold of CNS neurons for the vertebrates: the developing Xenopus laevis spinal cord. Dev Neurobiol 72(4):575–584

Rybak IA, Shevtsova NA, Lafreniere-Roula M et al (2006) Modelling spinal circuitry involved in locomotor pattern generation: insights from deletions during fictive locomotion. J Physiol 577:617–639

Shevtsova NA, Talpalar AE, Markin SN et al (2015) Organization of left-right coordination of neuronal activity in the mammalian spinal cord: insights from computational modelling. J Physiol Lond 593(11):2403–2426

Teka WW, Upadhyay RK, Mondal A (2017) Fractional-order leaky integrate-and-fire model with long-term memory and power law dynamics. Neural Netw 93:110–125

Yan CG, Yang Z, Colcombe SJ et al (2017) Concordance among indices of intrinsic brain function: Insights from inter-individual variation and temporal dynamics. Sci Bull 62(23):1572–1584

Yang Z, Zhang D, Rocha MV et al (2017) Prescription of rhythmic patterns for legged locomotion. Neural Comput Appl 28(11):3587–3601

Zhong G, Chen L, Jiao Z et al (2018) Locomotion control and gait planning of a novel hexapod robot using biomimetic neurons. IEEE Trans Control Syst Technol 26(2):624–636

Zhou Y, Yamamoto M, Engel JD (2000) GATA2 is required for the generation of V2 interneurons. Development 127(17):3829–3838